Magnetic Properties of Unique Apollo 17 Soil 70051. Yang Liu[1], James R. Thompson [2], Lawrence A. Taylor[1], and Jaesung Park[1] [1]Planetary Geosciences Institute, Dept. of Earth & Planetary Sciences, Univ. of Tennessee, Knoxville, TN 37996, [2]ORNL, Oak Ridge, TN 37831 & Dept. of Physics & Astronomy, Univ. of Tennessee, Knoxville, TN 37996.

Introduction: Lunar dust, the <20 μm portion of the Moon's regolith, posed several unanticipated problems during the Apollo Missions. With our plans for returning humans to the Moon, it is paramount to address these issues. For example, an embarrassing problem involved the fact that *none of the 'Million-dollars rock boxes'* built at Oak Ridge National Lab remained *sealed* at the vacuum of the Moon – i.e., *they all leaked* exposing the lunar samples to terrestrial air - because of the ubiquitous dust. Dust caused breathing problems for the astronauts upon their return to the Lunar Module – is this dust toxic to humans? Furthermore, the extreme abrasiveness of the lunar soil and dust impaired movement of joints in tools and instruments, as well as on astronaut's suits. Obviously, the lunar dust problem needs to be mitigated [1].

A myriad of nanophase metallic Fe grains (np-Fe^0) in the impact glass of agglutinates in the soil [2-4] presents unusual and interesting properties, including ferromagnetism, which can be used for dust abatement – e.g., a brush with a magnet attached. Therefore, it is obvious that we must investigate the magnetic properties of this finest portion of the lunar regolith.

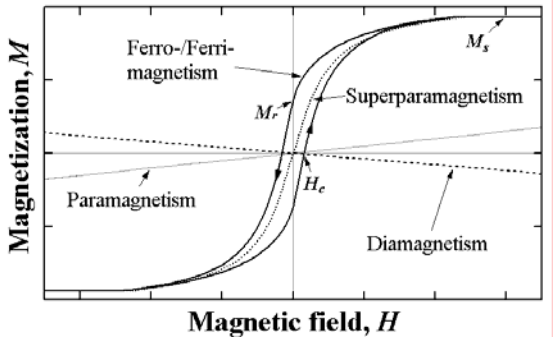

Fig. 1.Illustration of materials with different magnetic behaviors.

Background: The magnetic behavior of materials can be classified into five major groups: diamagnetism, paramagnetism, ferromagnetism, ferrimagnetism, and antiferromagnetism (Fig. 1, [e.g. 5-6]). Diamagnetic substances such as quartz and water show a negative magnetization when exposed to a magnetization field. Paramagnetic materials such as pyrite and biotite exhibit a weak positive magnetization. At room temperature, the moment generated by the field is roughly proportional to the field H. Ferro- and ferrimagnetic materials typically display similar "S"-shaped M-H curves. Their response is often hysteretic, as illustrated by the "hysteresis loop" in Fig. 1. The important parameters include the saturation magnetization (M_s), the residual magnetization (M_r) when the applied magnetic field is zero (H = 0), and coercivity (H_c) that is the reverse field needed to reduce the magnetization to zero after saturation. When the size of *isolated* (non-interacting) ferromagnetic particles decrease into the range of nanometers, their magnetic behavior becomes super-paramagnetic (~30 nm for Fe^0), meaning that the material becomes magnetically reversible and both M_r and H_c decrease to zero. Antiferromagnetic materials (such as ilmenite and ulvöspinel) generally display a linearly increasing magnetization, similar to a paramagnetic material.

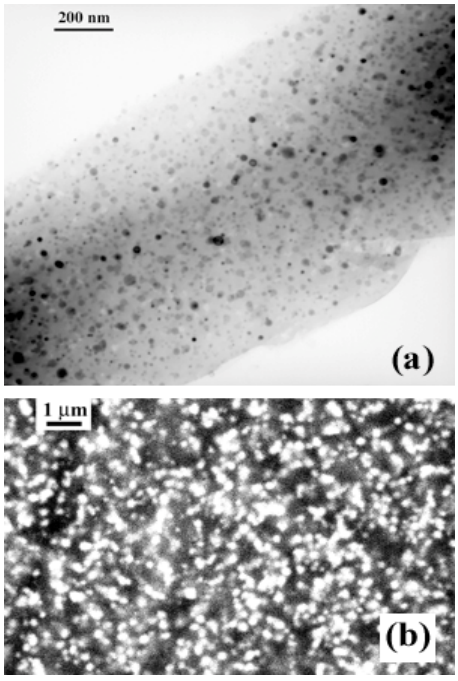

Fig. 2. LAG simulants from [7-8]. (a) TEM image of simulant LAG-s. Dark sports are metallic iron. (b) SEM picture of simulant LAG-b. Bright spheres are iron particles. Note the wide range of grain sizes.

Method: We used a Quantum Design MPMS-7 SQUID-based magnetometer at ORNL to obtain the magnetic moment m(H). The <45 μm portion of previously unstudied Apollo 17 soil 70051 was measured, as were several lunar soil simulants: 1) the most common lunar regolith simulant, JSC-1; and 2) our synthesized simulants with metallic iron particles (np-

Fe^0 in LAG-s and larger grains size in LAG-b from [7-8]). JSC-1 was produced from a basaltic tuff [9] and contains <0.5 wt% Fe-Ti oxides and ~1 wt% Cr-spinel [10], which contribute to its magnetic properties. Our simulant LAG-s with binary components (SiO_2-FeO) contains <50 nm metallic iron particles (Fig. 2a) while LAG-b with five components (SiO_2-Al_2O_3-CaO-MgO-FeO), contains Fe^0 particles with sizes < 500 nm (Fig. 2b).

Results: The magnetization of all samples shows typical S-shape curves, but also contain a near-linear paramagnetic signal at H >11 kOe. The latter signal increases as *T* is reduced, suggesting that it originates from non-metallic Fe in minerals and dissolved in

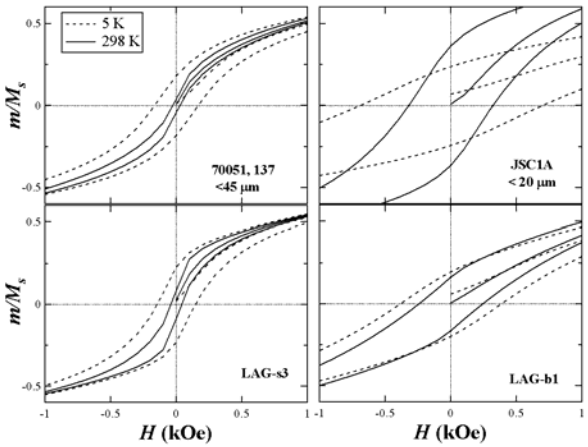

Fig. 3. Magnetization curves after subtracting the paramagnetic signals.

glass. After subtracting the paramagnetic signals, the magnetization curves at 298 K and 5 K are shown in Fig. 3. Sample 70051 and LAG-s3 have a narrow hysteresis loop at 298 K, indicating the strong contribution from np-Fe^0 particles. Sample 70051 also contains small amount of Fe-Ti oxides and Cr-spinel [11], which contribution to the magnetization is small. The similar S-shape curve of JSC-1 is probably a result of the Fe-Ti oxides and Cr-spinel. For the other three samples, the saturation magnetization at 298 K is used to calculate the metallic iron content: 0.77 wt% for sample 70051, 1.9-2.3 wt% for LAG-s, ~1.3 wt% for LAG-b. The metallic iron content and the initial susceptibility (at -100 to 100 Oe) of sample 70051 (28×10^{-4} emu·g^{-1}·Oe^{-1}) are not dissimilar from other lunar soils [e.g. 12-16].

Discussion: Figure 4 shows a comparison of lunar rocks/soil with the simulants. The positive correlation of lunar samples and simulants in Fig. 4 is possibly related to the iron grain size. The <45 μm portion of sample 70051 has a high abundance of agglutinitic glass [11]. The np-Fe^0 grains in agglutinitic glass that are generally <50 nm [2-4]. The size of metallic-iron

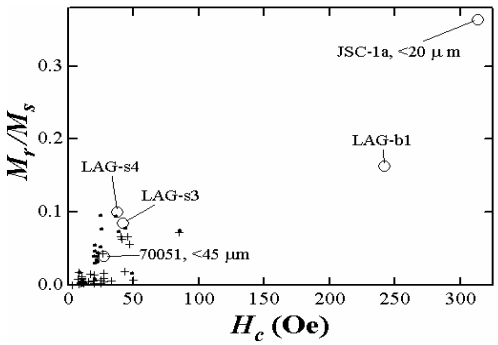

Fig. 4. The fractional remanent magnetization versus the coercive field of lunar rocks/soils with simulants. Small dots are measurements on lunar soils and small pluses are lunar rocks from [12-16].

particles increases from LAG-s to LAG-b (Fig. 2). Thus, for materials with nanometer iron grains that are small enough to be single domain, their M_r/M_s and H_c increases with the iron grain size, as expected from fundamental principles. Finally, we note that the observed magnetic hysteresis provides an additional mechanism for heating when the materials are subjected to intense RF power, as with high power microwave radiation. This potential source of heating will be assessed.

In summary, the simulant LAG-s successfully approximates the nanophase iron in lunar soil in grain size and magnetic properties. The thermal energy generated by alternating magnetic field can be estimated. New insight into the magnetic characteristics of these samples provides a firmer basis for possible dust mitigation processes.

References: [1] Taylor L. A. et al. (2005) *1st Space Explor. Conf., AIAA*. [2] Keller L. P. and McKay, D. S. (1993) *Science, 261*, 1305-1307. [3] Keller L. P. and McKay D. S. (1997) *Geochim. Cosmochim. Acta, 61*, 2331-2341. [4] Wentworth S. J. et al. (1999) *Meteor. Planet. Sci., 34*, 593-603. [5] Buschow K. H. J. and De Boer F. R. (2003) *Physics of Magnetism and Magnetic Materials*. pp. 182. [6] Fuller M. (1987) *Methods Expei. Phys., 24*, 303-471. [7] Liu Y. et al. (2005) *Meteor. Planet. Sci., 40, Suppl.*, A94. [8] Liu Y. et al. (2005) Space Resources Roundtable VII: LEAG Conf., LPI. *LPI Contr. 1287*, 61. [9] McKay D.S. et al. (1992) *Space IV, ASCE*, 857-866. [10] Hill E. et al. (2006) *ASCE 2006*. [11] Mellin M. et al. (2006) *LPSC XXXVII*, this volume. [12] Nagata T. et al. (1973) *LPSC IV*, 3019-3043. [13] Pearce G. W. et al. (1973) *LPSC IV*, 3045-3076. [14] Nagata T. et al. (1974) *LPSC V*, 2827-2839. [15] Pearce G. W. et al. (1974) *LPSC V*, 2815-2826. [16] Pearce G. W. and Chou C.-L. (1977) *LPSC VIII*, 669-667.